Microscopic Origins of the Anomalous Melting Behavior of Sodium under High Pressure

Hagai Eshet,[1,*] Rustam Z. Khaliullin,[1,2,†] Thomas D. Kühne,[3,4] Jörg Behler,[5] and Michele Parrinello[1]

[1]*Department of Chemistry and Applied Biosciences, ETH Zürich, and Facoltà di Informatica, Istituto di Scienze Computazionali, Università della Svizzera Italiana, via G. Buffi 13, 6900 Lugano, Switzerland*
[2]*Physical Chemistry Institute, University of Zürich, Winterthurerstrasse 190, 8057 Zürich, Switzerland*
[3]*Institute of Physical Chemistry, Johannes Gutenberg University Mainz, D-55128 Mainz, Germany*
[4]*Center for Computational Sciences, Johannes Gutenberg University Mainz, D-55128 Mainz, Germany*
[5]*Lehrstuhl für Theoretische Chemie, Ruhr-Universität Bochum, D-44780 Bochum, Germany*
(Received 31 October 2011; published 13 March 2012)

X-ray diffraction experiments have shown that sodium exhibits a dramatic pressure-induced drop in melting temperature, which extends from 1000 K at $\sim$30 GPa to as low as room temperature at $\sim$120 GPa. Despite significant theoretical effort to understand the anomalous melting, its origins are still debated. In this work, we reconstruct the sodium phase diagram by using an *ab initio* quality neural-network potential. Furthermore, we demonstrate that the reentrant behavior results from the screening of interionic interactions by conduction electrons, which at high pressure induces a softening in the short-range repulsion.

Sodium, a prototype simple metal at ambient conditions, exhibits unexpected complexity under high pressure [1–6]. At ambient conditions, sodium crystallizes in the body-centered cubic (bcc) structure, which transforms to the face-centered cubic (fcc) phase upon compression to 65 GPa [7]. At 105 GPa, the fcc phase undergoes a transformation to the *cI*16 phase—a distorted variant of the bcc structure [2,8]. Further compression results in the formation of a large variety of complex phases [3–6], the existence of which is quite intriguing. However, the focus of this work is one of the most striking features of the sodium phase diagram—the anomalous melting curve. Diffraction measurements have revealed a maximum in melting temperature around 1000 K at $\sim$30 GPa followed by a pressure-induced drop, which extends to nearly room temperature at $\sim$120 GPa [1] and over the stability regions of three solid phases [Fig. 1(a)]. This anomaly implies that in this range the liquid is denser than the solid.

Although previous *ab initio* studies [9–14] have reproduced the reentrant melting behavior of sodium, the physical origin of this anomaly still remains unclear. The hypothesis of structural and electronic transitions in liquid sodium proposed in one of the studies [10] has not been confirmed by other authors [9].

It is important to point out that due to the high computational cost of *ab initio* molecular dynamics (MD) all simulations so far reported [9–12] have used small simulation cells and estimated melting temperatures (T_m) by heating the solid phase until it melts. In such simulations, the absence of nucleation centers and fast heating schedules delay melting relative to the thermodynamic coexistence point, and, therefore, only an upper bound on T_m can be obtained. A proper reconstruction of the melting curve requires comparing the free energies of the liquid and solid

phases and involves long ($\sim$ 10 ns) MD simulations on large systems ($\sim 10^3$ atoms). Performing such simulations with direct *ab initio* methods is at present computationally too expensive. Although several authors [13,14] have demonstrated that simplified models can also reproduce the anomalous melting behavior, the relation of these models to the actual physical interactions in sodium has remained unclear.

In a previous work [15], we have shown that a neural-network (NN) potential [16,17] for sodium based on well-converged Perdew-Burke-Ernzerhof [18] density functional calculations retains the accuracy of *ab initio* simulations at a highly reduced computational cost. The ability of the NN potential to reproduce numerous *ab initio*
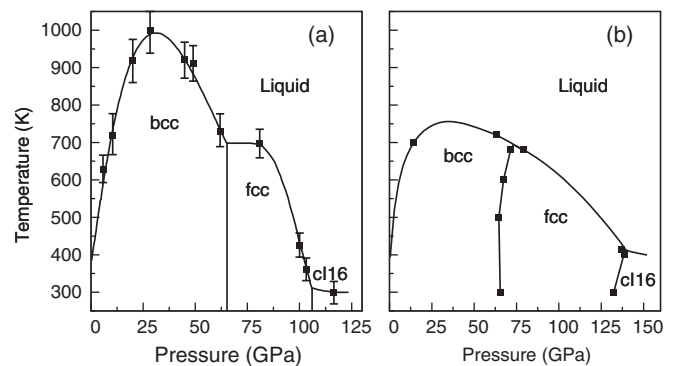

FIG. 1. Sodium phase diagram. (a) The squares represent experimentally measured melting points. The lines show tentative phase boundaries [1]. (b) Theoretical results based on the NN potential. The squares represent coexistence points computed with thermodynamic integration. The lines show coexistence curves traced by integrating the Clausius-Clapeyron equation (see [19]).

and experimental properties of the solid and the liquid phases in the pressure range up to 140 GPa has been demonstrated in Ref. [15]. Additionally, Supplemental Fig. 1 [19] shows the high accuracy of the NN potential in reproducing the *ab initio* energies for liquid sodium structures along MD trajectories in the relevant *P-T* range. Furthermore, Supplemental Fig. 2 [19] demonstrates that the "heat-until-it-melts" melting curve calculated with the NN potential is in good agreement with that obtained from *ab initio* simulations [12].

Here we utilized the NN potential to construct the sodium phase diagram. The phase diagram shown in Fig. 1 was calculated by locating points of equal chemical potential for each pair of phases in the *P-T* plane. This was done in three steps (see Refs. [19,20]). First, we calculated the Helmholtz free energy of each pair of phases by thermodynamic integration using the Einstein crystal and the Lennard-Jones potential as the reference systems [21]. In the next step, the chemical potentials were evaluated by integrating the free energy as a function of the density. Finally, the coexistence lines were traced by integrating the Clausius-Clapeyron equation using the predictor-corrector scheme of Kofke [22]. The total simulation time required to model the phase diagram amounts to ~50 ns, clearly demonstrating the computational advantage of the NN approach in comparison with the direct *ab initio* simulation.

The NN potential captures the experimentally observed sequence of the solid-state phase transitions bcc → fcc → *cI*16 and the regions of stability of each phase. The shape of the melting curve with the maximum around 30 GPa is also correctly reproduced. The comparison of NN and density-functional theory transition pressures at zero temperature (Fig. 6 in Ref. [15]) as well as the heat-until-it-melts melting curves obtained from NN and *ab initio* simulations (Supplemental Fig. 2 [19]) show that the quantitative errors in the coexistence lines can be attributed to inaccuracies of the density functional and not to the errors of the NN fitting. Supplemental Fig. 2 [19] also demonstrates that T_m obtained with a nonequilibrium approach is overestimated compared to the proper thermodynamic calculation. To the best of our knowledge, this is the first phase diagram calculated from a high-quality *ab initio* method.

To verify the existence of structural and electronic transitions in the liquid phase, which has been suggested before to explain the anomalous melting [10], we evaluated the order parameter introduced in Ref. [10] to monitor structural changes in the liquid sodium (see [19]). Our calculations do not reveal any significant variations in the structure of liquid in the 0–140 GPa range along the calculated melting curve [Supplemental Fig. 3(a) [19]]. In addition, the electronic density of states calculated with density-functional theory for liquid structures collected from NN-driven MD simulations does not exhibit the opening of a pseudogap observed before [10] [Supplemental Fig. 3(b) [19]]. Discrepancies between our results and Ref. [10] can be attributed to the explicit

inclusion of the 2*s* and 2*p* electrons in the present calculations. It has been shown that these states play an important role in determining properties of liquid at high pressure [12].

While the NN simulations reproduce adequately the sodium melting curve, the physical origins of its reentrant behavior are difficult to extract. To this effect, we constructed a density-dependent pair potential based on the jellium model for the conducting electrons. According to this model, the ionic structure of a metal can be replaced, to a first approximation, by a uniform positively charged background, while conduction electrons can be treated as a uniform electron gas. The granularity of sodium is then introduced at the level of two-body interactions by immersing two Na atoms in such a jellium and calculating the energy as a function of the interatomic distance (see [19]). The effect of the pressure is taken into account by varying the density of the electron gas ρ_e according to the NN equation of state. By doing so, we retraced a time-honored idea used to construct effective potentials describing screening effects in metals by linear response theory [23]. Here, we used a nonlinear approach, since it is expected that nonlinear screening effects become important as the ions are brought closer to each other by the applied pressure.

We found that the two-body effective potential obtained from the jellium model is well reproduced by a sum of the repulsive Yukawa potential and the oscillatory Friedel term (Supplemental Fig. 4 [19]) [24,25]:

$$\phi(r) = \frac{A \exp(-k_0 r)}{r} + \frac{B \cos[2k_F(r - r_0)]}{r^m},$$

where A, B, k_0, r_0, and m are density-dependent fitting parameters and k_F is the true (i.e., not fitted) Fermi wave number (see Supplemental Table 1 [19]). This analytical form of the potential is inspired by a linear screening theory [23] and reflects the nature of physical interactions in metallic sodium, in which the direct Na-Na repulsion is screened by the free-electron gas. In particular, the oscillatory term has its origin in the sharpness of the Fermi surface.

MD simulations based on the effective pair potential reproduce semiquantitatively the maximum in the melting curve (Fig. 2). The potential is also remarkably accurate in describing the radial distribution functions (RDFs) of the liquid for pressures up to 100 GPa (Supplemental Fig. 5 [19]). We thus believe that this effective density-dependent two-body potential is able to capture the physics of the problem and can be used to shed light on the origin of the anomalous melting behavior. It is worth mentioning that the validity of this potential is limited to the region of pressures below about 120 GPa, because beyond this region electrons are promoted to the *d* states and the simple free-electron two-body model is no longer appropriate.

We examined the effect of two different parts of the effective potential on the melting curve. First, we
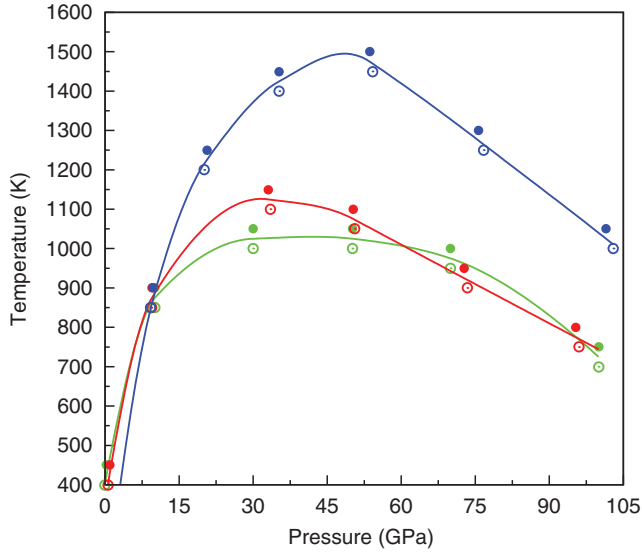
FIG. 2 (color). The heat-until-it-melts curves obtained with the NN potential (green), effective pair potential based on the jellium model (red), and repulsive wall of the effective pair potential (blue). The points below 90 GPa are obtained by melting the bcc phase and the points above 90 GPa by melting the fcc phase. To obtain the curves, the temperature was increased in 50 K increments with open and solid circles showing the solid and liquid states, respectively.

considered the Yukawa part of the potential and, second, the repulsive wall of $\phi(r)$. The latter was constructed by truncating the total potential at its first minimum and shifting it so that both the energy and force are zero at the truncation point [26]. We found that the Yukawa potential cannot reproduce the reentrant melting behavior. On the contrary, the melting curve obtained with the repulsive wall
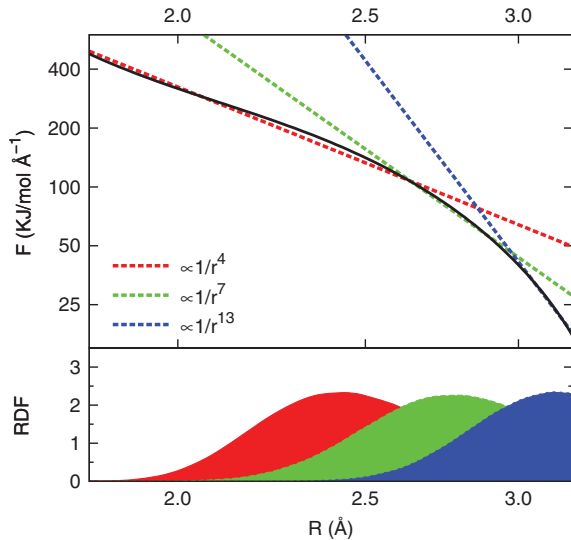

FIG. 3 (color). Upper panel: Interatomic forces in the region of the repulsive wall of the effective pair potential (black solid line). Lower panel: RDF of liquid sodium along the melting curve at $\sim$10 (blue), $\sim$30 (green), and $\sim$90 GPa (red).

exhibits a maximum similar to that obtained with the full potential (Fig. 2). This observation suggests that it is the short-range repulsive part of the potential that provides the origin of the anomalous melting (see [19] for a detailed pressure decomposition analysis that confirms this conclusion).

The log-log plot of the interatomic force in the region of the repulsive potential wall shown in Fig. 3 supports this point of view. It is seen that there is a large change of the slope as the potential changes from $1/r^{12}$ to a much softer $1/r^3$ behavior (i.e., the slope changes from $1/r^{13}$ to $1/r^4$ in Fig. 3). The lower panel of the same figure shows the RDFs obtained at different pressures along the melting line. It demonstrates that at low pressure only the steep part of the repulsive wall is sampled, whereas at higher pressure the softer short-range part of the potential starts influencing the atomic interactions. Since softening the potential lowers the melting temperature [27,28], we argue that the softening of the repulsive interactions in sodium at high pressure is the origin of the observed anomaly.

Our results fit well into the existing theories of metals that predict an increase of screening with density [29,30]. They are also in agreement with theoretical predictions that
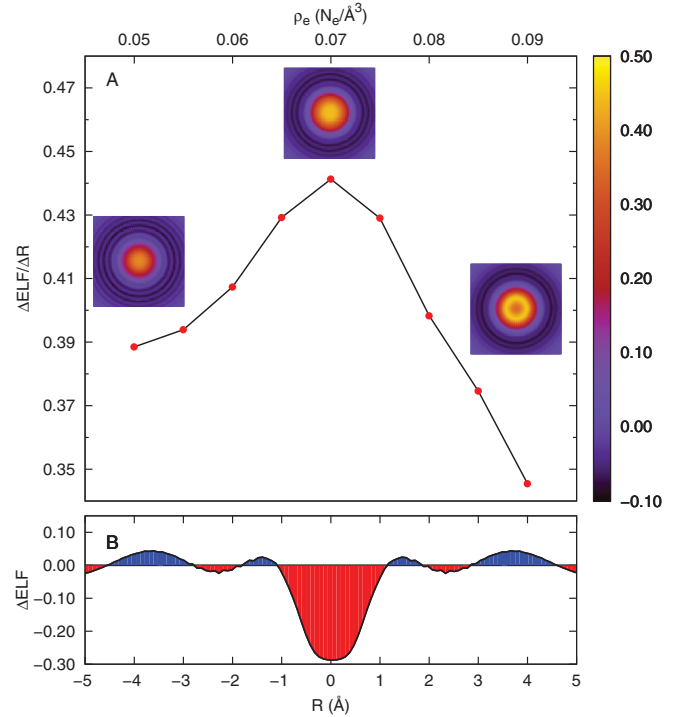

FIG. 4 (color). (a) Pressure dependence of the derivative of the ELF at the center of the Na-Na bond with respect to interatomic distance taken at the distance of the nearest neighbor in the bcc lattice. For comparison, the maximum of T_m is around $\rho_e \approx 0.0615$ Å^{-3}. The insets show 2D plots of the same derivative in the plane perpendicular to the Na-Na bond for ρ_e: 0.05 ($\sim$ 20), 0.07 ($\sim$ 45), and 0.09 Å^{-3} ($\sim$ 90 GPa). (b) Difference between the high-pressure and low-pressure values of ELF in the direction perpendicular to the Na-Na bond: ΔELF $\equiv$ ELF(90 GPa) $-$ ELF(25 GPa).

certain softening in simple model potentials can result in anomalous melting [31]. Our work demonstrates, for the first time, that the screening-induced softening can lead to a dramatic decrease in the melting temperature of a real material.

In order to understand the electronic origin of the softening effect, we examined the behavior of the electron localization function (ELF), which is widely used to analyze the nature of chemical bonds (see Methods) [32,33]. Figure 4(a) shows the behavior of the derivative of the ELF with respect to the interatomic distance, which can be taken as a measure of the softness of the bond. The derivative closely follows the behavior of the melting curve, dramatically decreasing at high pressure. It is instructive to compare the ELFs at low and high pressures. Figure 4(b) shows that electrons localized in the Na-Na bond move to the outer regions as pressure increases. The tendency of electrons to move from the bonding regions to the interstitial regions at high pressure has already been noted [34,35].

In conclusion, the insight into the electronic and structural properties of sodium obtained in this work offers a new consistent explanation of the anomalous melting behavior of Na. We demonstrated that the observed dramatic drop in the melting temperature can be attributed to the density dependence of the conduction electrons screening, which induces a softening of the interatomic potential at short range. Our preliminary results indicate that similar softening effects are responsible for the reentrant melting in other alkali metals such as lithium and potassium. These findings have immediate implications for explaining behavior of other metals and alloys.

———

*hagai.eshet@gmail.com
†rustam@khaliullin.com

[1] E. Gregoryanz, O. Degtyareva, M. Somayazulu, R.J. Hemley, and H.K. Mao, Phys. Rev. Lett. **94**, 185502 (2005).

[2] M.I. Mcmahon, E. Gregoryanz, L.F. Lundegaard, I. Loa, C. Guillaume, R.J. Nelmes, A.K. Kleppe, M. Amboage, H. Wilhelm, and A.P. Jephcoat, Proc. Natl. Acad. Sci. U.S.A. **104**, 17 297 (2007).

[3] E. Gregoryanz, L.F. Lundegaard, M.I. Mcmahon, C. Guillaume, R.J. Nelmes, and M. Mezouar, Science **320**, 1054 (2008).

[4] Y.M. Ma, M. Eremets, A.R. Oganov, Y. Xie, I. Trojan, S. Medvedev, A.O. Lyakhov, M. Valle, and V. Prakapenka, Nature (London) **458**, 182 (2009).

[5] A. Lazicki, A.F. Goncharov, V.V. Struzhkin, R.E. Cohen, Z. Liu, E. Gregoryanz, C. Guillaume, H.K. Mao, and R.J. Hemley, Proc. Natl. Acad. Sci. U.S.A. **106**, 6525 (2009).

[6] L.F. Lundegaard, E. Gregoryanz, M.I. McMahon, C. Guillaume, I. Loa, and R.J. Nelmes, Phys. Rev. B **79**, 064105 (2009).

[7] M. Hanfland, I. Loa, and K. Syassen, Phys. Rev. B **65**, 184109 (2002).

[8] K. Syassen, in *High Pressure Phenomena, Proceedings of the International School of Physics*, edited by R.J. Hemley, G.L. Chiarotti, M. Bernasconi, and L. Ulivi (IOS, Amsterdam, 2002), pp. 266–268.

[9] E.R. Hernandez and J. Iniguez, Phys. Rev. Lett. **98**, 055501 (2007).

[10] J.Y. Raty, E. Schwegler, and S.A. Bonev, Nature (London) **449**, 448 (2007).

[11] L. Koci, R. Ahuja, L. Vitos, and U. Pinsook, Phys. Rev. B **77**, 132101 (2008).

[12] A. Yamane, F. Shimojo, and K. Hoshino, J. Phys. Soc. Jpn. **77**, 064603 (2008).

[13] M. Martinez-Canales and A. Bergara, J. Phys. Chem. Solids **69**, 2151 (2008).

[14] S.V. Lepeshkin, M.V. Magnitskaya, and E.G. Maksimov, JETP Lett. **89**, 586 (2009).

[15] H. Eshet, R.Z. Khaliullin, T.D. Kühne, J. Behler, and M. Parrinello, Phys. Rev. B **81**, 184107 (2010).

[16] J. Behler and M. Parrinello, Phys. Rev. Lett. **98**, 146401 (2007).

[17] J. Behler, Phys. Chem. Chem. Phys. **13**, 17 930 (2011).

[18] J.P. Perdew, K. Burke, and M. Ernzerhof, Phys. Rev. Lett. **77**, 3865 (1996).

[19] See Supplemental Material at http://link.aps.org/supplemental/10.1103/PhysRevLett.108.115701 for further information.

[20] R.Z. Khaliullin, H. Eshet, T.D. Kühne, J. Behler, and M. Parrinello, Phys. Rev. B **81**, 100103 (2010).

[21] D. Frenkel and B. Smit, *Understanding Molecular Simulation: From Algorithms to Applications* (Academic, Orlando, 2001).

[22] D.A. Kofke and P.T. Cummings, Mol. Phys. **92**, 973 (1997).

[23] N.W. Ashcroft and N.D. Mermin, *Solid State Physics* (Saunders College, Philadelphia, 1976).

[24] H.R. Leribaux and M.H. Boon, Phys. Rev. B **11**, 2412 (1975).

[25] A. Paskin and A. Rahman, Phys. Rev. Lett. **16**, 300 (1966).

[26] J.D. Weeks, D. Chandler, and H.C. Andersen, J. Chem. Phys. **54**, 5237 (1971).

[27] W.G. Hoover, S.G. Gray, and K.W. Johnson, J. Chem. Phys. **55**, 1128 (1971).

[28] D.A. Young, *Phase Diagrams of Elements* (University of California, Berkeley, 1991).

[29] J. Hafner and V. Heine, J. Phys. F **13**, 2479 (1983).

[30] J. Hafner, J. Phys. Condens. Matter **2**, 1271 (1990).

[31] S. Prestipino, F. Saija, and G. Malescio, J. Chem. Phys. **133**, 144504 (2010).

[32] A.D. Becke and K.E. Edgecombe, J. Chem. Phys. **92**, 5397 (1990).

[33] B. Silvi and A. Savin, Nature (London) **371**, 683 (1994).

[34] B. Rousseau and N.W. Ashcroft, Phys. Rev. Lett. **101**, 046407 (2008).

[35] J. Yang, J.S. Tse, and T. Iitaka, J. Phys. Condens. Matter **22**, 095503 (2010).